Porvali, A.; Agarwal, V.; Lundström, M.

REE(III) recovery from spent NiMH batteries as REE double sulfates and their simultaneous hydrolysis and wet-oxidation

Published in:
Waste Management

DOI:
10.1016/j.wasman.2020.03.042

Published: 15/04/2020

Document Version
Publisher's PDF, also known as Version of record

Please cite the original version:
Porvali, A., Agarwal, V., & Lundström, M. (2020). REE(III) recovery from spent NiMH batteries as REE double sulfates and their simultaneous hydrolysis and wet-oxidation. *Waste Management*, *107*, 66-73.
https://doi.org/10.1016/j.wasman.2020.03.042

Waste Management 107 (2020) 66–74

Contents lists available at ScienceDirect

Waste Management

journal homepage: www.elsevier.com/locate/wasman

REE(III) recovery from spent NiMH batteries as REE double sulfates and their simultaneous hydrolysis and wet-oxidation

A. Porvali, V. Agarwal, M. Lundström *

Aalto University, School of Chemical Engineering, Department of Chemical and Metallurgical Engineering, P.O. Box 16200, Aalto 00076, Espoo, Finland

ARTICLE INFO

Article history:
Received 11 November 2019
Revised 12 February 2020
Accepted 30 March 2020

Keywords:
Cerium
Wet oxidation
Selective dissolution
Spent NiMH batteries

ABSTRACT

Efficient recovery of REEs present in the battery waste is a modern problem that has proven to be difficult to solve in an efficient manner. The raw material investigated in the current study is mixed alkaline rare earth element (REE) double sulfate (DS) precipitate, originating from the sulfuric acid leachate of nickel-metal hydride battery (NiMH) waste. Typically, REE can be precipitated as a mixture of REE double sulfates, however the real challenge is the separation of REEs from each other's into pure fraction. The study elucidates the process by which the DS are transformed into hydroxides with simultaneous in-situ conversion of Ce(III) to Ce(IV) by air. Air flow rate (0–1 L/h), temperature (30–60 °C), liquid-solid ratio (L/S, 12.5–100 g/L), 3REE/NaOH mol ratio (1–1.6) and time (60–240 min) were varied in the study of oxidation and double sulfate conversion. Best oxidation achieved was 93% along near-complete dissociation of double sulfate matrix (52767 ppm Na reduced to 48 ppm Na). After parameter optimization, a larger batch was produced to conduct selective dissolution of REE(III) into HNO_3 media, leaving concentrated impure $Ce(OH)_4$ as the end product.

1. Introduction

Rare earth elements (REEs) are mainly found in bastnäsite, loparite, monazite, and xenotime ores and used in wide variety of modern life applications. Cerium is a common REE element, and occupies nearly half of the total REEs composition in bastnäsite at Mountain Pass, California, USA and ~43% of total REEs in monazite ore at Nangang, Guangdong, China (Bleiwas and Gambogi, 2013). Cerium or cerium containing compounds are extensively used in glasses, catalyst, polishing, batteries and alloys and for example in the end-of-life, nickel-metal-hydride (NiMH) battery waste contain significant amount of cerium (~0.4–5.5 wt.%). During battery recycling process, NiMH battery waste leaching can be carried out by using several lixiviants, such as HCl, HNO_3 and H_2SO_4, sulfuric acid leaching being the most common. (Rodrigues and Mansur, 2010) The resultant leach solution contains valuable elements like: REEs, Zn, Ni, Co, Fe, Mn, Cd and Al (Zhang et al., 1999).

Selective separation of REEs from other metal ions can be carried out by double salt precipitation ($REENa(SO_4)_2$) using sodium sulfate (Na_2SO_4) as a precipitating agent, Eq. (1) (Innocenzi et al., 2017,Abreu and Morais, 2010,Moeller and Kremers, 1945). However, all REEs (La, Ce, Pr, Nd) end up to the formed-REE double salts as mixed crystals, because of similar physical and chemical properties of the light REEs, and further separation among these trivalent REEs is laborious (Porvali et al., 2018).

$$REE^{3+} + Na^{+} + 2SO_4^{2-} + xH_2O \rightarrow REENa(SO_4)_2 \cdot xH_2O \quad (1)$$

Cerium is one of the unique REEs which can exist in a stable form in both +3 and +4 oxidation states in aqueous solutions. Due to drastically different chemical properties between the trivalent and tetravalent REEs (Krishnamurthy and Gupta, 2015), this property of cerium has been commonly utilized in order to separate cerium as Ce(IV) from the other trivalent REEs by oxidizing Ce(III) to Ce(IV). In acidic solutions, strong chemical oxidants are required to oxidize Ce(III) to Ce(IV) (McNeice et al., 2019) while in alkaline solution, Ce(III) can be readily oxidized to Ce(IV) by first converting mixture of REE double salts to hydroxide. This is done by dissolving the double sulfate, causing a near-immediate hydrolysis of REE cations. The necessary basic conditions are maintained by adding the required stoichiometric amount of NaOH to neutralize the acid borne in hydrolysis of aqueous REE ions, Eqs. (2)–(5). Simultaneously, $Ce(OH)_3$ is oxidized by air or oxygen purging, Eq. (6) (Dan et al., 2014). The E-pH behavior of Ce is highlighted in studies of *Hayes et al.* and *Yu et al.*, showing how strongly basic conditions influence the oxidation of Ce(III) (Hayes et al., 2002,Yu et al., 2006).

---

* Corresponding author.
E-mail address: mari.lundstrom@aalto.fi (M. Lundström).

https://doi.org/10.1016/j.wasman.2020.03.042
0956-053X/© 2020 The Authors. Published by Elsevier Ltd.

$$REENa(SO_4)_2 \cdot xH_2O \rightarrow REE^{3+} + Na^{+} + 2SO_4^{2-} + xH_2O \quad (2)$$

$$REE^{3+} + 3H_2O \rightarrow REE(OH)_3 + 3H^{+} \quad (3)$$

$$3H^{+} + 3NaOH \rightarrow 3Na^{+} + 3H_2O \quad (4)$$

In total, the suggested conversion reaction would be according to Eq. (5)

$$REENa(SO_4)_2 \cdot xH_2O + 3NaOH \rightarrow REE(OH)_3 + 2Na_2SO_4 + (x+3)H_2O \quad (5)$$

$$2\mathrm{Ce(OH)_3} + \frac{1}{2}\mathrm{O_2} + \mathrm{H_2O} = 2\mathrm{Ce(OH)_4(s)} \quad (6)$$

Ce(III) can be oxidized to Ce(IV) with several methods such as oxidative roasting (Wang et al., 2013) and the use of strong oxidative reagents (McNeice et al., 2019). *Rabie et al.* investigated removal of cerium from the lanthanide oxide cake, obtained from Egyptian monazite and reported that cerium oxidation was increased with the addition of bleaching powder (hypochlorite) (Rabie et al., 1998). Dissolution of REE(III) was favored more in nitric acid than in hydrochloric acid solutions in the presence of bleaching powder. However, higher REE(III) dissolution and oxidation of cerium were obtained using mixed solution of both acids (1:1). *Chi et al.* proposed a two-step leaching method to separate cerium from bastnäsite calcine using hydrochloric acid (Chi et al., 2006). In the first step, dilute hydrochloric acid was used to separate trivalent REEs from cerium and in the second step, concentrated hydrochloric acid was used in the presence of hydrogen peroxide as a reducing agent to produce a cerium rich leachate (recovery ~ 85.3%).

It can be seen from literature that many studies have been reported on selective separation of Ce(IV) from other REE(III) by combining precipitation and leaching in some manner, however in most of the cases either strong, harmful or expensive chemical reagents were used for the cerium oxidation, selective dissolution or solvent extraction. In addition, most of the investigations were performed on primary ores like bastnäsite and monazite. The application of wet air oxidation on the REE double salt originating from NiMH battery wastes is still missing in the open literature. It is evident that the increasing pressure for REE recovery from waste streams, such as NiMH batteries, emphasizes the need for improved knowledge of the further purification of the rare earth double salt. Wet air oxidation has been considered as an environment friendly and cost effective method, where the use of hazardous chemicals, energy and material consumption are minimal (Zou et al., 2014). In the case of cerium, oxygen from air can be directly utilized by purging the basic Ce-containing solution with air, while operating at appropriate basicity. *Zou et al.* studied the wet air oxidation of Ce(III) originating from synthetic REE hydroxides prepared from REE nitrate solution and reported that ~ 97% of the Ce(III) oxidation could be achieved under the tested conditions (Air flow rate, FR = 3 L min^{-1}, T = 80 °C, t = 4 h and pH = 13) (Zou et al., 2014), proving that it is possible to achieve good Ce oxidation with mixed REE hydroxide.

In general, recovery of Ce from mixed REE double sulfates originating from different sources has been investigated before. In an investigation, ceric hydroxides were prepared by treating Ce(III) synthetic solution with sodium sulfate to form cerium double salt followed by hydroxide conversion by adding NaOH (Jia et al., 2000). However, final oxidation of Ce(III) was achieved by adding hydrogen peroxide, an expensive and strong oxidant. Furthermore, no consideration was given to the influence of liquid to solid ration (L/S) in aqueous hydroxide solution, a factor that was investigated in the present study. *Abreu et al.* employed a double sulfate precipitation and Ce oxidation (Abreu and Morais, 2010). The REEs originated from monazite sulfuric acid leach liquor from which the double sulfates were obtained. The double sulfates were then converted to hydroxides and dissolved in hydrochloric acid, from which Ce was precipitated by addition of a strong oxidant, $KMnO_4$ and Na_2CO_3, and with careful control of pH. *Um and Hirato* also investigated a similar scheme of REE double sulfate processing, however the oxidation was done separately from the hydroxide conversion (Um and Hirato, 2016). They also used polishing powders as a raw material which are rich in Ce, having a significantly different REE composition than that of NiMH batteries. This is important as it may influence the entrapment of elements within the Ce matrix.

In this work, a practical approach for the separation of Ce(IV) and other REE(III) present in NiMH battery waste is investigated, Fig. 1. This approach includes sulfuric acid leaching of NiMH waste, double salt precipitation of REEs, in-situ wet air oxidation of cerium and hydroxide conversion of REEs. The hydroxides are then acid-treated to recover trivalent REEs. The current study is differentiated from study of *Abreu et al.* by utilizing simultaneous double sulfate to hydroxide conversion and wet oxidation (Abreu and Morais, 2010) and from the wet-oxidation study of *Zou et al.* as the present study utilized REE double sulfates instead of nitrates as the source of REEs. Moreover, the present study is differentiated from the study of *Um and Hirato* by utilizing a more dilute NaOH concentrations along with simultaneous conversion and wet oxidation (Um and Hirato, 2016). The prior studies have also omitted

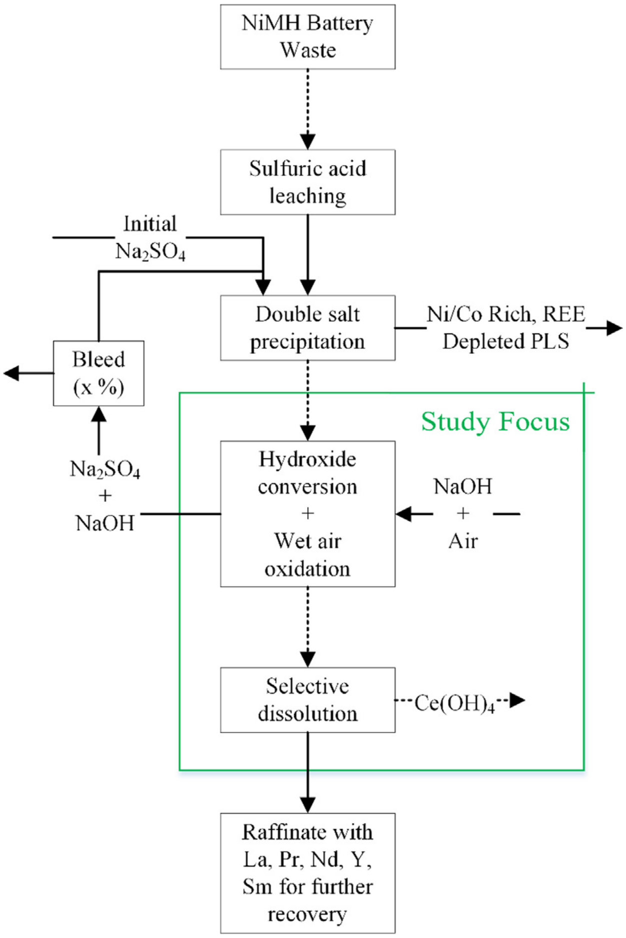

Fig. 1. Block diagram for the separation and recovery of Ce(IV) and REE(III) from NiMH battery waste. Dashed lines relate to the solid fractions, and solid lines to the solutions. Green outline presents the focus of the current study.

the study of the effect of liquid to solid ratio (L/S) on REE double sulfate conversion to hydroxides. In present study, the focus is on investigation and optimization of the parameters that affect the conversion of the double sulfate, oxidation of cerium and selective dissolution of trivalent REEs, including the L/S ratio. The scope of the current study is shown in the diagram, Fig. 1. It is noteworthy that the sodium used for double salt precipitation can be back circulated from the hydroxide conversion step to allow the minimization of the chemical consumption (Porvali et al., 2019). After the conversion and oxidation, REE(III) are selectively dissolved over Ce(IV). In selective dissolution of REE(III) hydroxides, several acids could potentially be used. However, in sulfuric acid, the solubility of REEs is limited (La solubility *ca.* 23.7 g/L in H_2SO_4 vs. > 100 g/L in HNO_3). In contrast, the chlorine ions in HCl can act as a reductant, facilitating the dissolution of $Ce(OH)_4$ while releasing Cl_2 gas. Another hypothetical alternative could be a weak acid with sufficiently high pK_a which would naturally facilitate dissolution at appropriate pH range. For present study, nitric acid was chosen due to high solubility of REE nitrates, especially $La(NO_3)_3$. Since the selectivity of the process is in part based on pH, careful neutralization of the trivalent hydroxides is necessary (Mioduski et al., 1989).

2. Materials and methods

2.1. Raw materials

The procedure by which double sulfates, prepared from spent NiMH batteries, were obtained is described in the supplementary materials S1.1. The chemical contents of the produced double salt mixture was determined by total dissolution by using ICP-OES (Thermo Fisher Scientific iCAP 6500 DUO, USA) and ICP-MS (Thermo Fisher Scientific iCAP Qc, USA). The characterization was performed three times for three different random samples. The results of the chemical analysis and the coefficient of variation (CV) of the double salt is presented in Table 1. It can be seen that the starting raw material contained 34.14 wt.% of REEs in the double sulfate, with a mixture of different REEs and Ni (357 ppm) and Mn (141 ppm) as the main impurity metals originating from the battery waste. CV for the main REEs (La-Nd) were determined to be 5.51–6.33%.

2.2. Wet oxidation and conversion

A 100 mL jacketed glass reactor was utilized in the oxidation experiments. The reactor was connected to a water bath with a thermostat and thermometer. The reactor was covered with a necked lid with a locking mechanism. The necks on the lid were sealed with polymer corks, all but one through which a Teflon pipe was inserted for gas purging. In the reactor, a small PTFE coated magnet was used as a source of agitation. The reactor lied atop of VWR magnetic stirring plate.

A stock solution of appropriate NaOH concentration (7.37 g/L NaOH, VWR pellets Analar NORMAPUR 99.2%) was prepared for the oxidation experiments. Compressed air was used as oxidant during the double salt dissolution and Ce oxidation. The experiments were planned as a single parameter variation experiments, Table 2 (Experimental Series A). In this work, L/S ratio is defined as grams of double salt per L of NaOH solution. A total amount of 16 experiments was performed for the matrix. Some experiments were randomly repeated in order to verify the repeatability of results.

Prior the injection of the sample into solution, the solution was pre-heated to target temperature, while air was being purged into the solution. After the experiment, stirring and purging was stopped and a sample was retrieved with a pipette. The sample was vacuum filtrated, rinsed with distilled water from the filter paper into a volumetric flask containing 50 mL of 2 M H_2SO_4 solution, which was diluted to mark of 100 mL, resulting in 1 M H_2SO_4 solution. The solution sample was divided into two parts. Ce(IV) content was determined from one part whereas the other part was subjected to oxidative treatment, followed by total Ce determination by titration. The pH of the leach solution (NaOH filtrate) was measured after each experiment by using Mettler-Toledo S210 EasyLab pH meter, connected to Mettler-Toledo InLab Expert PRO (ISM) pH electrode.

2.3. Ce(IV) titration

The Ce(IV) content of each sample after the experiment was determined by titration. Ammonium iron sulfate hexahydrate ($(NH_4)_2Fe(SO_4)_2{\cdot}6H_2O$, Sigma-Aldrich, ACS Reagent 99%) was used as a titrant. The titrant was standardized against a ceric sulfate solution ($Ce(SO_4)_2{\cdot}4H_2O$, 98%, VWR EMSURE). Ferroin solution (0.2 wt.%) prepared from o-phenanthroline monohydrate (ACS Reagent, >99.5%) was used as an indicator color. The total Ce content of the sample was also determined by titration by utilizing a method demonstrated by Willard and Young in 1928, a procedure which is described elsewhere in detail (Willard and Young, 1928). 2.5 g/L silver nitrate solution ($AgNO_3$, >99% Honeywell (Titration)) was used as a catalyst source and ammonium persulfate ($(NH_4)_2S_2O_8$, Merck, 99%) was used as an oxidant. With each sample, titration was repeated at minimum twice to confirm continuous repeatability of the method.

2.4. Crystallinity of the hydroxides

In Experimental Series B, crystallinity of the obtained hydroxides was investigated at T = 30 and 70 °C, *3NaOH/REE* = 1.2, *FR* = 0.4 L/min, *L/S* = 25 g/L and t = 2 h. Furthermore, it was investigated whether the double sulfates could be detected when *3NaOH/REE* = 0.5. X-ray diffraction (XRD, X'Pert Pro MPD Powder, USA, equipped with PIXcel1D detector, Co Kα source operated at 40 kV, 40 mA, along with Fe beta filter and no monochromator) and HighScore 4.0 software was utilized in the analysis of the obtained diffractograms of powders.

2.5. Selective dissolution

The hydroxide powder used in these experiments was produced by performing large-scale (3 L) conversion and oxidation with the optimal parameters (*L/S* = 25 was used, along with *FR* = 1 L/min, *3NaOH/REE* = 1.6, T = 60 °C and t = 2 h) obtained from the

Table 1
The chemical analysis of the double salt raw materials as ppm. * = ICP-MS. ** = ICP-OES.

	La*	Ce*	Pr*	Nd*	Y*	Sm*	Ni**	Co*
Mean	162,667	108,133	11,500	37,567	510	212	377	70.4
CV (%)	5.51	6.29	6.07	6.33	10.41	6.16	6.41	8.14
	Mn*	**Al***	**Fe****	**Zn***	**Na****	**K****	**S****	
Mean	144.7	30.6	20.0	29.8	52,767	6632	157,000	
CV (%)	6.19	17.51	1.31	16.67	2.79	0.28	2.08	

Table 2
Experimental Series A for single parameter variation experiments. Values indicated by * were kept constant while the other parameter was varied.

3NaOH/REE (mol/mol)	T (°C)	Flow rate (L/min)	Time (min)	L/S ratio (g/L)
1*	30*	0	60*	12.5
1.2	40	0.4*	90	25*
1.4	50	0.6	120	50
1.6	60	1	240	100

optimization experiments. 75 g of double salt originating from sulfuric acid leaching of NiMH battery waste was added into a 3 L reactor. The obtained precipitate was characterized with SEM-EDX, ICP-MS and its Ce oxidation degree by titration.

Selective dissolution (Experimental Series C) was performed as an investigation to the effect of pH on the solubility of the mixed, oxidized REE hydroxide powder. First, the consumption of H^+ ions was measured by using a 25 mL burette for titration. $REE(OH)_3$ sample (5 g) was utilized. The acid addition on precipitate was continued until the buffering effect disappeared and pH of 1.7 was reached. The obtained precipitate was also analyzed with SEM-EDX and by ICP-MS.

3. Results and discussion

3.1. Wet oxidation and conversion

The double salts were dissolved in NaOH solution in Experimental Series A, where the dissolved REEs were hydrolyzed and precipitated as REE hydroxides. All the constant parameter levels in leaching were chosen based on principle of least harsh conditions. For temperature, 30 °C was chosen as a middle point. *Zou et al.* reported successful oxidation experiments with synthetic hydroxide powders obtained from REE nitrates at 40 °C, but they did not investigate the oxidation at a lower temperature (Zou et al., 2014). Initial NaOH concentration was limited to *3NaOH/REE* = 1.0. This resulted in different initial pHs at different L/S ratios, however, if the reaction were to proceed to completion the final pH should be similar between different L/S ratios. Air flow rate (FR) was the minimum i.e. 0.4 L/min given by the rotameter. The minimum time used was 60 min. The reaction assumed to take place was Eq. (5 and 6). However, in the case of Ce, the reactions may be much more complicated. Once its liberation as an ion from the double salt occurs, there are several depictions of its oxidation by different oxidants. Variation can be found in the literature, as the resulting precipitate is sometimes presented as $Ce(OH)_4$ or $CeO_2{\cdot}2H_2O^{23}$. $Ce(OH)_4$ is often referred to as $CeO_2{\cdot}2H_2O$, which is stoichiometrically identical. However, structurally $CeO_2{\cdot}2H_2O$ must be distinguished from anhydrous CeO_2, which is extremely difficult to dissolve with any strong mineral acid alone (Um et al., 2011).

Temperature was varied between 30 and 60 °C and the results are presented in Fig. 2A. It was expected that temperature will affect the experiment in several ways: dissolution kinetics of the double salt, oxidation kinetics and also solubility of $O_2(g)$ (Zou et al., 2014). Oxidation was shown to improve as a function of temperature. Surprisingly, at $T = 30$ °C, an oxidation degree of 76% was already achieved only in 1 h. The best results was achieved with $T = 50$ °C and 60 °C (oxidation *ca.* 90%), where the result plateaued and no further oxidation was observed. This is in contrast to result by Zou et al., who demonstrated continuous improvement in oxidation throughout 40–80 °C, but in a longer oxidation time of 4 h. This may indicate that the detected "plateau" in the current study is caused by the interdependency of oxygen solubility and higher reaction kinetics brought by an increase in *T*. The measured final pH decreased as a function of *T* (from 11.97 to 11.72), which is a sign of progressing hydrolysis of REEs.

To study the optimum chemical use, the ratio of NaOH vs. REE was investigated, Fig. 2B. The oxidation degree was shown to increase slightly but linearly with increasing NaOH concentration. The best oxidation (81%) was obtained at *3NaOH/REE* = 1.6. Increase in oxidation between the experiments may be attributed to kinetic improvements to the hydrolysis of REEs due to higher driving force, i.e. having higher supersaturation, Eq. (5). The oxidation of the Ce will be kinetically depended on the dissolution of the double salts and their subsequent hydrolysis, where the increase of initial NaOH concentration may provide some advantage. However, the effect of NaOH/REE ratio was not equally significant as the effect of temperature.

The oxidation was investigated also as a function of time, Fig. 2C. It was observed that increase in reaction time from 60 to 120 min improved the oxidation result, however longer reaction times did not increase the observed oxidation degree, while the pH was observed to decrease consistently as a function of time (pH = 11.97 → 11.5).

The effect of air purging rate was investigated with and without purging, shown in Fig. 2E. Since air was purged into the solution prior the start of each experiment, it was expected that the solution would be saturated with the gas molecules present in air. Oxygen solubility depends on both pH of the solution and temperature (Zou et al., 2014), which can limit the oxidation kinetics. In the used center point of temperature (30 °C) the solubility of O_2 in H_2O is 1.18326 mmol/L (Miyamoto et al., 2014). This was calculated to be *ca.* decade lower compared to that of the mol amount of Ce (solubilized 19.3 mmol/L). This shows that the pre-saturated solution could not cause immediate oxidation of all the Ce, but that new O_2 molecules were needed via continuous air purging. This was verified by a comparative experiment without any air purging, with the oxidation as low as 12.7%. With flow rates 0.4–1.0 L/min the oxidation degree improved to 76–81%. It is also possible that this increase between 0.4 and 1.0 L/min can be attributed to increase in mixing efficiency as the flow rate was rather large for the size of the reactor.

L/S Ratio affects the kinetics of the DS dissolution and oxidation, shown in Fig. 2D. By supplying more solid contents to identical solution volume, there is a reduction in reaction rate, shown as a decrease in the overall oxidation, Fig. 2F. This conclusion is supported by the high final pH of the solution (pH = 11.6 → 12.6) in the case of *L/S* = 100. The dissolution of DS and precipitation of $REE(OH)_3$ has not occurred yet, which would subsequently cause reduced base consumption and explain higher final pH at higher L/S ratios. Even though the percentage of oxidized species decreased with increasing *L/S* (Fig. 2D), the actual mass of oxidized Ce increased as a function of *L/S*. This result is plotted Fig. 2F, where it can be seen that there is no linear dependency between the data points, but the results suggest second-order polynomial fitting. This result, combined with the increase in final pH as a function of increasing *L/S* ratio, strongly suggests that there exists constraints on double salt dissolution and hydrolysis of the dissolved REEs which is limiting the oxidation of Ce. At higher solid contents an increase in reaction time may be needed as initially the high pH of the solution will impact, even drastically, the solubility of O_2 gas.

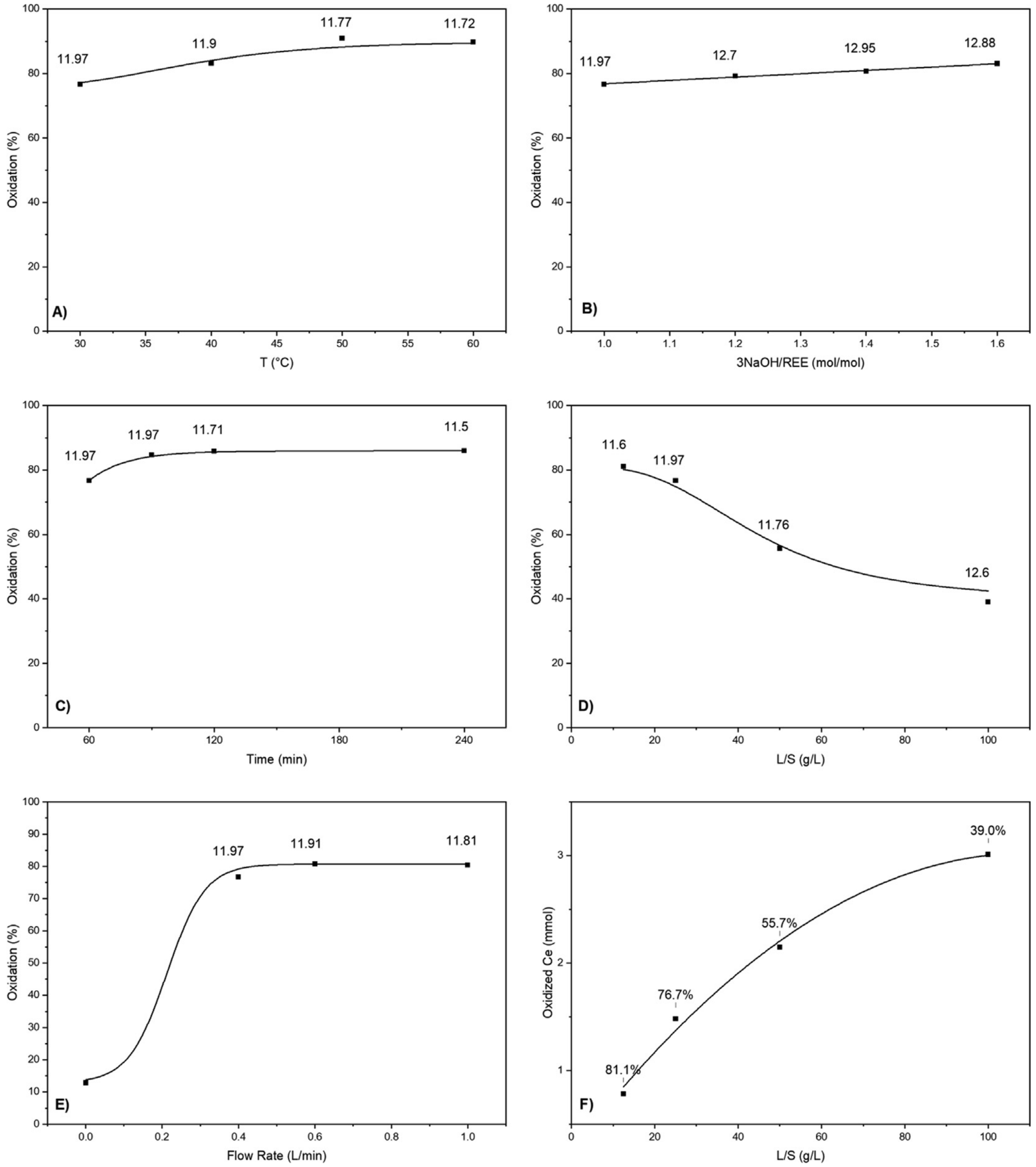

Fig. 2. Oxidation of Ce(III) to Ce(IV) during double salt conversion – oxidation experiments (Experimental Series A). Oxidation results as a function of A) temperature (°C), B) 3NaOH/REE, C) time (min), D) L/S ratio and E) air flow rate. The final pH is reported above data points. Constants: T = 30 °C, t = 60 min, 3NaOH/REE = 1.0, L/S = 25 g/L, FR = 0.4 L/min. F) The amount (mmol) of oxidized Ce as a function of L/S. (T = 30 °C, FR = 0.4 L/min, t = 60 min, 3NaOH/REE = 1.0. Oxidation degree reported above the data point.

It could also be possible that the observed decrease in oxidation is due to limited solubility of double salts in the basic solution, which is being caused by the increase in SO_4^{2-} ion concentration according to Eq. (2). This would present significant hindrance in treating REEs in this manner as it would limit what would be a usable L/S.

The resulting precipitate in *L/S* = 100 was subjected to XRD, however, no peaks was observed, but just diffraction indicating amorphous background, and is therefore not presented here. The precipitate was also investigated with SEM-EDS (Fig. 3) and original double sulfates was observed, accompanied by large amount of REE hydroxides. The double salts exhibited the typical hexagonal crystallographic structure with larger particle size (Perles et al., 2005), Fig. 3A. This may partially explain the high final pH: the dissolution reaction had not progressed to the end, and perhaps the increase in dissolved SO_4^{2-} content limits the dissolution of the double sulfates in the basic solution. With EDX (Fig. 3B), it was possible to consistently find particles with significant sulfur content, ranging from 3.5 atomic.% to 6.9 atomic.%. (scan sites 1–5). This further supports the view that the oxidation degree decreases due to the unreacted double sulfates. The hypothesis of unreacted double sulfates are further supported by SEM micrographs, shown in Supplementary materials S1.2. Micrographs of the L/S = 100 experiment were obtained at two points of time: immediately after the experiment, and at a later time after experiment. The purpose of the investigation was to investigate the presence of different particle sizes in the materials. These micrographs show that throughout the experiment, precipitation has had different drivers. It was possible to find many small crystals, agglomerated together as shown in Fig. S3, appearing to be in size 1–2 μm. This is typical to nucleation-driven crystallization, occurring in systems of high supersaturation. Not only that, but it was also possible to find extremely large crystals, shown as well in the micrograph Fig. S3.

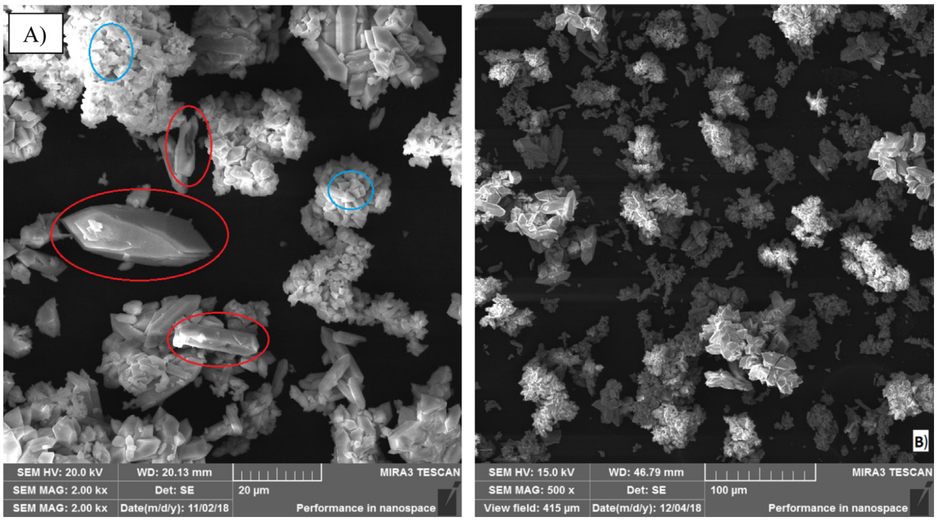

Fig. 3. A) Secondary electron (SE) micrograph of hexagonal double salts and amorphous hydroxides from L/S = 100 experiment on carbon tape. Crystals surrounded by red circles were identified as double salts, and crystals surrounded by blue circles as hydroxides. B) Small magnification overview of the mixed hydroxide, devoid of double sulfate, obtained from optimal parameter experiment (T = 60 °C, 3NaOH/REE = 1.6, FR = 1 L/min, t = 120 min.

This is indicative of reduced driving force for crystallization, which is a result of decreased driving force, i.e. decreased supersaturation. Furthermore, there were signs of crystallization occurring at even lower supersaturation, as it was possible to find crystals that exhibited spiral crystal growth patterns, Fig. S4. These micrographs are shown in supplementary materials S1.2

After the conversion experiments, the optimal parameters were used in a large scale experiment (Section "Selective Dissolution"). 75 g of double salt originating from sulfuric acid leaching of NiMH battery waste was added into a 3 L reactor. Oxidation degree was measured to be 93%, which was the best result achieved in the current study. In total, 40 g of dry powder was obtained after reaction, filtration and drying. The powder was analyzed by ICP-MS, Table 3. Low Na content (52767 ppm vs. 48.2 ppm, before and after transformation) indicates that most of the double salts had dissociated and was removed during the dissolution and conversion – however, the amount of sulfur remaining was still substantially high. The only source of sulfur in conversion stage was the double sulfate itself – and although sodium was mostly removed, sulfur remained in the final powder. At present, it was not possible to propose a hypothesis for high sulfur content (157000 ppm vs 24900 ppm, before and after transformation), but it is evident that Na was effectively removed during the wet oxidation and conversion stage i.e. during transformation from double sulfate. The result is similar to the result of *Abreu et al.* who obtained 0.9 wt.% SO_4^{2-} content at T = 70 °C (Abreu and Morais, 2010). Moreover, they had a high residual sulfate content in the product at T = 30 °C, suggesting that T = 60 °C that was utilized in present study may explain why the sulfur content in the present study was 2.49 wt.%.

The hydroxide powder from the optimal parameter experiment was also subjected to SEM characterization, shown in Fig. 3B. Large crystals and their agglomerates, assumed to be REE hydroxides, could be observed to have been formed, partially explaining the easy filterability.

In all the conversion-oxidation experiments of Experimental Series A, it was noted that the produced precipitate was easily filterable powder and did not present any significant gel-like characteristics. This is not typical behavior as REE hydroxide precipitation from aqueous solution results in gel-like precipitate (Shkol'nikov, 2009). This could be due to the low NaOH concentrations that were utilized in this study, limiting the supersaturation levels (Myerson, 2002). Similar easy-to-filter behavior was also shown by *Neckers and Kremers* in 1928 from hydrolysis of ceric phosphates (Neckers and Kremers, 1928). The lack of gelatinous character can be taken as an advantage of the application of conversion and wet oxidation method on REE double salts.

Furthermore, another advantage of the presently suggested method has been shown by a prior study that in NaOH conversion of REE double sulfates (Eq. (1)), the resulting sodium sulfate – sodium hydroxide solution could potentially be recirculated back to double salt precipitation. This would reduce the consumption of Na, and simultaneously ensure appropriate stoichiometric excess of Na ions (Na/REE = 4/1) in the REE double sulfate precipitation (Kul et al., 2008,Porvali et al., 2019).

3.2. Crystallinity of the hydroxides

Characterization of the mixed hydroxide mass is not generally possible with XRD. This is due to the amorphous structure of the precipitates, caused by short reaction time at low temperature. The reaction time should be increased along with temperature and NaOH conc. in order to obtain crystalline structure due to the aging phenomena (Abreu and Morais, 2010). *Abreu et al.* reported having obtained crystalline REE$(OH)_3$ from double salts at *3NaOH/REE* = 1.25 and T = 70 °C, however they did not provide

Table 3
The hydroxide powder composition, reported in ppm.

Al	**Ce**	**Co**	**Fe**	**K**	**La**	**Mn**
33.9	187,000	91.7	34.1	189	264,000	215
Na	**Nd**	**Ni**	**Pr**	**S**	**Sm**	**Y**
48.2	76,200	621	21,300	24,900	389	797

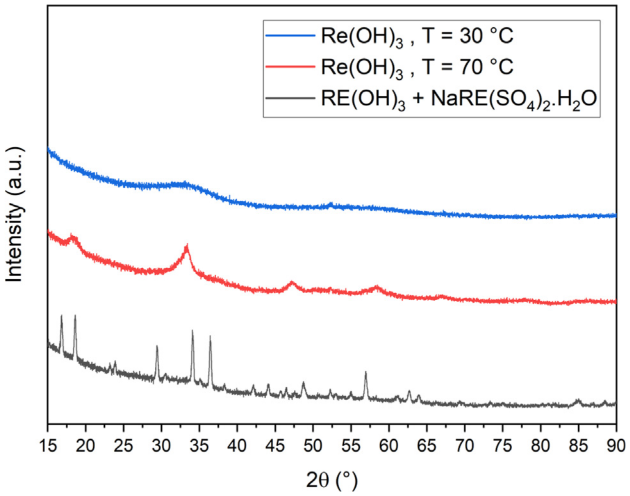

Fig. 4. A composite of separate diffractograms. The first is from the center point experiment (Experimental Series A), second from the 70 °C, 2 h (Experimental Series B) and third from the 3NaOH/REE = 0.5 (Experimental Series B).

an XRD diffractogram of the product to support their claim (Abreu and Morais, 2010). To that end, it was investigated whether crystalline REE(OH)$_3$ can be obtained by using similar parameters.

In the Experimental Series B, the process of double salt conversion and oxidation was attempted. It can be clearly seen that some diffraction peaks that could correspond to REE hydroxides become more apparent at T = 70 °C. The resulting diffractograms clearly show the product was not crystalline. The peaks are wide and the background is curved in a way that resembles the REE(OH)$_3$ at 30 °C. *Zhang et al.* have shown that similar quality of crystallinity can be obtained at 100 °C from nitrate media, but for highly ordered structure a higher temperature up to 600 °C is required (Zhang et al., 2004). Finally, in order to ascertain that whether it is possible to see the double salt remnants in XRD at all, *3NaOH/REE* = 0.5 was used and the resulting precipitate was analyzed by XRD. The result in Fig. 4 clearly shows the peaks associated with the double salt, however, it is also possible to note the curved background which is caused by the amorphous precipitates.

3.3. Selective dissolution of the hydroxides

After the preparation of the hydroxides (Table 3), at first, selective dissolution of La, Pr and Nd hydroxides from Ce(IV) hydroxide was investigated with careful HNO$_3$ addition (Experimental Series C). Pale yellow color indicating the dissolution of Ce^{4+} was observed at pH = 1.7–1.9 after 1 h equilibration, corresponding to *ca. ca.* 10.9 mmol HNO$_3$ consumption per gram of the mixed hydroxide. The observed pH for detecting the pale yellow color was lower (1.7–1.9) than that suggested (2.2–2.6) by *Mioduski et al.* (Mioduski et al., 1989). As a result of selective dissolution, clear enrichment of Ce could be achieved. However, even at optimized pH (1.7), both minor La and Pr, in addition to Nd, remained in the cerium precipitates as impurity elements, Table 4. Overall, La content was reduced from 264000 ppm to 15600 ppm (94.1% reduction), Pr from 21300 ppm to 2200 ppm (89.7% reduction), Nd from 76200 ppm to 7875 ppm (89.7% reduction). This is most likely due to the fact that the pH of the solution was decreased slowly and gradually, avoiding momentary decrease of pH below the desired target that could result if the acid was added all at once. Ce was enriched from 187000 ppm to 451500 ppm (241% increase). Interestingly, sulfur was also enriched, from 24900 ppm to 40150 ppm. This could be indicative of sulfur being present in the precipitate (Table 3) in such species that cannot be dissolved by the dilute nitric acid either. However, it is more likely that the Ce is associated with the Ce(IV) matrix and other trivalent REEs as well. After selective dissolution, 5 g of mixed hydroxide was reduced to 1.49 g, equaling to 97–98% extraction of La, Pr and Nd when calculated based on data in Table 3 and Table 4. Ce extraction was 28%, and S 52%. Some Ce extraction is expected, as all the Ce(III) would be expected to dissolve. Furthermore, at titration end point of pH = 1.7 the amount of added acid is also excessive, and the titration was only stopped when yellow color was detected. However, in this manner it is proven that the Ce matrix contains locked-in impurities, including some trivalent REEs as well as quite large fraction of the original sulfur content, most likely as sulfates, which can't be removed without an additional total dissolution – precipitation cycle. The cerium enriched particles obtained from selective dissolution were also investigated by means of SEM-EDX. The presence of sulfur is clearly indicated, and the EDX supports the results presented in Table 4. The sulfur is distributed evenly to different investigated zones, as shown in Table 4. However, the results do not reveal the nature of the sulfur present in the precipitates. *Abreu et al.* suggested the presence of RE$_2$SO$_4$(OH)$_4$·H$_2$O, however only at insufficient base quantities (Abreu and Morais, 2010). In the current study, the REE/S ratio (mol/mol) was 5.04 after hydroxide conversion and 2.72 after selective dissolution. The investigated zone 4 was still covered by epoxy and is excluded.

The results show high enrichment (up to 54 times) of the Ce from the NiMH battery based double sulfate precipitate to Ce precipitate – however it also highlights the potential challenges that lie in separation of Ce by the process approach proposed in this paper. High sulfur content is particularly problematic and warrants further investigation. These results indicate that sulfur is strongly associated with Ce instead of the rest of the REEs. It might be advantageous to first dissolve the whole mixed hydroxide and then precipitate the Ce directly by increasing the pH. Another option would be the complete dissolution of the mixed hydroxide precipitate which would ensure that entrapped atoms are released, and Ce precipitation could be attempted directly by increasing the pH of the solution. Sulfuric acid could potentially be utilized in the re-dissolution as we have now shown that the amount of Na is

Table 4
The chemical analysis of the produced precipitate in acid treatment, Experimental Series B. Results are reported in ppm. EDX-results of the select zones, reported in (atom.%/atom.%)·10^2. Initial D.S. calculated from ICP-MS results (Table 1).

La (ppm)	Ce (ppm)	Pr (ppm)	Nd (ppm)	Sm (ppm)	Y (ppm)	Na (ppm)	S (ppm)
15,600	451,500	2200	7875	54	73.5	47.1	40,150
EDX Results	La/Ce	Ce/Ce	Pr/Ce	Nd/Ce	Y/Ce	S/Ce	
Initial D.S.	147	100	10.5	33.7	0.78	606	
1	2.71	100	0.78	0.39	0.00	20.2	
2	4.42	100	0.00	0.34	0.00	18.4	
3	3.82	100	1.27	2.04	0.00	19.6	
5	2.30	100	0.00	0.00	0.00	20.3	

not significant, and double sulfate precipitation could be avoided. The method presented here highlights the potential and limitations of using wet-air oxidation with double sulfates as the source of REEs in selective recovery of Ce.

4. Conclusions

The paper presents an investigation on alternative route for Ce recovery and enrichment from the NiMH battery waste by using a robust method not yet investigated in battery recycling. The advantage of the presented process route is that it allows the use of less aggressive and expensive chemicals (sulfuric acid, NaOH, air and nitric acid) for the separation of Ce compared to the state-of-art processes or literature. It also has the potential to incorporate the recycling of the produced Na_2SO_4 solution into double salt precipitation. The proposed method consist of double sulfate precipitation of REEs from NiMH PLS, followed by hydroxide conversion and their subsequent wet oxidation by air, and further selective dissolution of trivalent REEs from the tetravalent Ce hydroxide.

Conversion of mixed REE double salts into REE hydroxides and the simultaneous oxidation of trivalent Ce was investigated by adjusting several different parameters: L/S ratio (12.5–100 g/L), air flow rate (0–1 L/min), temperature (30–60 °C), 3NaOH/REE ratio (1–1.6) and time (60–240 min). It was found that L/S = 100 g/L resulted in slowing down of the conversion of the hydroxide, as indicated by high sulfur content (*ca.* 10 more than in the optimized experiment) of the resulting precipitate. This was judged to be due to decrease in dissociation of double salts, as was evident from SEM micrographs and EDX results which revealed presence of Na. This explains partially the low oxidation degree in relation to other studies using synthetic solutions as the raw material instead of DS produced from battery waste. Generally, oxidation degree of Cerium ranged from 82% to 93% throughout the experiments. It was shown that at high L/S ratio of 100, the double sulfate conversion was hindered, most likely due to decreased solubility caused by the dissolved sulfate ions.

Using the optimized conditions (T = 60 °C, t = 120 min, *L/S* = 25 g/L, *FR* = 1 L/min, *3NaOH/REE* = 1.6) a 3 L reactor was used to convert double salts to hydroxides and simultaneously oxidize Ce, resulting in 93% oxidation degree. Characterization of hydroxides was not possible with XRD due to its amorphous structure. However, with the help of the total dissolution, it was possible to ascertain that the amount of sodium was reduced to 48 ppm, indicating dissociation of double sulfates. However, impurities were still locked within the matrix of the intermediate product. This was evident once the precipitate was subjected to selective dissolution with nitric acid. Visually, it was observed that the solid tetravalent cerium appeared to remain stable until at least pH of 2 and that enrichment of Ce was observed (from 108133 ppm in double sulfate to 451500 ppm Ce in acid-treated hydroxide). 97–98% extraction of trivalent REEs was achieved, indicating that impurities still remained in the Ce-enriched precipitate.

Declaration of Competing Interest

The authors declare that they have no known competing financial interests or personal relationships that could have appeared to influence the work reported in this paper.

Acknowledgements

We would like to thank Dr. Fupeng Liu for assistance with a SEM micrograph (Fig. 4A) and the associated EDX analysis (Fig. 4A), and also for valuable suggestions in the selective dissolution part of the study. We would also like to thank the funding bodies: MineWEEE (grant number 7100/31/2016), and BATCircle (grant number 4853/31/2018), both funded by Business Finland (BF). The research was also supported by the Strategic Research Council at the Academy of Finland, project CloseLoop (grant number 303454). RawMatTERS Finland Infrastructure (RAMI) funded by Academy of Finland is also greatly acknowledged.

Appendix A. Supplementary material

Supplementary data to this article can be found online at https://doi.org/10.1016/j.wasman.2020.03.042.

References

Abreu, R.D., Morais, C.A., 2010. Purification of rare earth elements from monazite sulphuric acid leach liquor and the production of high-purity ceric oxide. Miner. Eng. 23, 536–540.

Bleiwas, D.I., Gambogi, J., 2013. Preliminary estimates of the quantities of rare-earth elements contained in selected products and in imports of semimanufactured products to the United States. USGS.

Chi, R., Li, Z., Peng, C., Gao, H., Xu, Z., 2006. Preparation of enriched cerium oxide from bastnasite with hydrochloric acid by two-step leaching. Metallur. Mater. Trans. B 37, 155–160.

Dan, Z., Ji, C., Deqian, L., 2014. Separation chemistry and clean technique of cerium (IV): A review. J. Rare Earths 32, 681–685.

Hayes, S.A., Yu, P., O'Keefe, T.J., O'Keefe, M.J., Stoffer, J.O., 2002. The phase stability of cerium species in aqueous systems i. e-ph diagram for the ce hclo 4 h 2 o system. J. Electrochem. Soc. 149, C623–C630.

Innocenzi, V., Ippolito, N.M., Michelis, I.D., Prisciandaro, M., Medici, F., Vegliò, F., 2017. A review of the processes and lab-scale techniques for the treatment of spent rechargeable NiMH batteries. J. Power Sources 362, 202–218.

Jia, J., Yan, C., Oh, J., Kim, C., Pyun, C., 2000. Preparation of ceric hydroxide through transformation of cerium compounds. Geosyst. Eng. 3, 81–83.

Krishnamurthy, N., Gupta, C.K., 2015. Extractive Metallurgy of Rare Earths. CRC Press.

Kul, M., Topkaya, Y., Karakaya, İ., 2008. Rare earth double sulfates from pre-concentrated bastnasite. Hydrometallurgy 93, 129–135.

McNeice, J., Kim, R., Ghahreman, A., 2019. Oxidative precipitation of cerium in acidic chloride solutions: part I - Fundamentals and thermodynamics. Hydrometallurgy 184, 140–150.

Mioduski, T., Hao, D.A., Luan, H.H., 1989. Separation of cerium from other lanthanides by leaching with nitric acid rare earth (III) hydroxide-cerium (IV) oxide mixtures. J. Radioanal. Nucl. 132, 105–113.

Miyamoto, H., Yampolski, Y., Young, C.L., 2014. IUPAC-NIST Solubility Data Series. 103. Oxygen and Ozone in Water, Aqueous Solutions, and Organic Liquids (Supplement to Solubility Data Series Volume 7). J. Phys. Chem. Ref. Data 43, 033102.

Moeller, T., Kremers, H.E., 1945. Observations on rare earth double sodium sulfate precipitation for separation of the terbium and yttrium earths. Ind. Eng. Chem. Anal. Ed. 17, 44–45.

Myerson, A.S., 2002. Handbook of Industrial Crystallization. Elsevier Science & Technology, Oxford.

Neckers, J., Kremers, H., 1928. Observations on the rare earths. Xxviii. The separation of cerium. J. Am. Chem. Soc. 50, 955–958.

Perles, J., Fortes-Revilla, C., Gutiérrez-Puebla, E., Iglesias, M., Monge, M.Á., Ruiz-Valero, C., Snejko, N., 2005. Synthesis, structure, and catalytic properties of rare-earth ternary sulfates. Chem. Mater. 17, 2701–2706.

Porvali, A., Agarwal, V., Lundström, M., 2019. Circulation of sodium sulfate solution produced during NiMH battery waste processing. Min., Metall. Explor. 36, 979–991.

Porvali, A., Wilson, B.P., Lundström, M., 2018. Lanthanide-alkali double sulfate precipitation from strong sulfuric acid NiMH battery waste leachate. Waste Manage. 71, 381–389.

Rabie, K., El-Hazek, N., Ali, M., El-Alfy, M., Aly, H., Zayed, M., 1998. Separation of cerium (III) from Egyptian monazite by oxidation to cerium (IV). In: Third Arab Conference on the Peaceful Uses of Atomic Energy, Damascus 9-13 Dec. 1996.

Rodrigues, L.E.O.C., Mansur, M.B., 2010. Hydrometallurgical separation of rare earth elements, cobalt and nickel from spent nickel–metal–hydride batteries. J. Power Sources 195, 3735–3741.

Shkolnikov, E.V., 2009. Thermodynamic characterization of the amphoterism of hydroxides and oxides of scandium subgroup elements in aqueous media. Russ. J. Appl. Chem. 82, 2098–2104.

Um, N., Hirato, T., 2016. A hydrometallurgical method of energy saving type for separation of rare earth elements from rare earth polishing powder wastes with middle fraction of ceria. J. Rare Earth. 34, 536–542.

Um, N., Miyake, M., Hirato, T., 2011. Dissolution of cerium oxide in sulfuric acid. In: Zero-Carbon Energy Kyoto 2010. Springer, pp. 165–170.

Wang, L., Yu, Y., Huang, X., Long, Z., Cui, D., 2013. Toward greener comprehensive utilization of bastnaesite: Simultaneous recovery of cerium, fluorine, and thorium from bastnaesite leach liquor using HEH (EHP). Chem. Eng. J. 215, 162–167.

Willard, H., Young, P., 1928. Ceric sulfate as a volumetric oxidizing agent. I. Preparation and standardization of solutions. Determination of calcium. J. Am. Chem. Soc. 50, 1322–1334.

Yu, P., Hayes, S.A., O'Keefe, T.J., O'Keefe, M.J., Stoffer, J.O., 2006. The phase stability of cerium species in aqueous systems II. The systems. Equilibrium considerations and pourbaix diagram calculations. J. Electrochem. Soc. 153, C74–C79.

Zhang, F., Yang, S., Chen, H., Yu, X., 2004. Preparation of discrete nanosize ceria powder. Ceram. Int. 30, 997–1002.

Zhang, P., Yokoyama, T., Itabashi, O., Wakui, Y., Suzuki, T.M., Inoue, K., 1999. Recovery of metal values from spent nickel–metal hydride rechargeable batteries. J. Power Sources 77, 116–122.

Zou, D., Chen, J., Cui, H., Liu, Y., Li, D., 2014. Wet air oxidation and kinetics of cerium (III) of rare earth hydroxides. Ind. Eng. Chem. Res. 53, 13790–13796.